Composite membranes with surface-modifying macromolecules for halogenated hydrocarbons removal from water in membrane extraction process

G.M. Nisola, A.B. Beltran[1], M.J. Park, R.E. Torrejos, J.G. Seo, S.-P. Lee, W.-J. Chung[*]

Department of Energy and Biotechnology (DEB), Energy and Environment Fusion Technology Center (E2FTC), Myongji University, Yongin City, Gyeonggi 449-728, South Korea, emails: ace.nisola@gmail.com (G.M. Nisola), mistof7@gmail.com (A.B. Beltran), mjpark1008@gmail.com (M.J. Park), reytorrejos@gmail.com (R.E. Torrejos), jeonggilseo@gmail.com (J.G. Seo), spleemju2012@gmail.com (S-P Lee), wjc0828@gmail.com (W-J Chung)

ABSTRACT

Flat sheet composite polysulfone (PSf) membranes blended with surface-modifying macromolecules (SMM) were prepared, characterized, and tested for halogenated hydrocarbons (HHC) (i.e. trichloroethylene, TCE) permeation and separation from water in an extractive membrane system. The fluorine end groups in SMMs facilitated its migration towards the membrane surface during membrane casting, whereas the polydimethylsiloxane component rendered the SMM organophilic which improved the surface affinity of the composite membrane towards TCE. Polydimethylsiloxane content in SMM, SMM content in PSf, and air-exposure of the casted blend solutions before membrane formation were found critical in obtaining an effective composite membrane. The presence of a selective SMM layer on the membrane surface was confirmed via contact angle measurement, Fourier-transform infrared spectrometry analysis, and field emission-scanning electron microscope. The most effective composite membrane (PSf with 15 wt% H-SMM and air exposed for 5 min before phase inversion) exhibited TCE flux values ranging between 640 and 1790 mg/m^{2}h when fed with TCE concentrations between 30 and 105 mg/L. Overall results demonstrate the potential use of the composite extractive membrane for the removal of hydrophobic organic contaminants like HHCs from aqueous streams.

Keywords: Composite membrane; Extractive membrane; Halogenated hydrocarbon; Surface-modifying macromolecule; Water purification

---

*Corresponding author.

[1]Chemical Engineering Department, De La Sale University Manila, 2401 Taft Avenue, Manila, 1004, Philippines.

1. Introduction

The prolific industrial use and disposal of halogenated hydrocarbons (HHCs) has led to their high environmental presence in surface water and groundwater. As organic contaminants with carcinogenic and mutagenic properties, HHCs removal is an utmost necessity [1]. Relevant treatment processes such as aeration, adsorption, ozonation, and advanced oxidation have been developed but all features certain limiting drawbacks for widespread application. Alternatively, organophilic membrane-based separations via selective permeation of hydrophobic HHCs from the bulk feed water have been performed in pressure-driven membrane systems such as pervaporation (PV) and membrane distillation [2–4]. A facile and efficient method yet rarely investigated is membrane extraction (ME), in which HHCs separation from water can be performed without external pressure requirement. The contaminant transport is driven by the concentration gradient across the membrane [5]. But as concentration gradient is a lower driving force than that of pressure, membranes must have enhanced transport properties (i.e. minimal membrane resistance) for maximum contaminant removal. A convenient method to obtain a suitable extractive membrane for HHCs is to fabricate a composite membrane with an extremely thin selective layer on its surface. A surface modification technique has been previously reported by using surface-modifying macromolecules (SMMs). At minimal blending concentration with a base polymer, SMMs with tailored functional groups (i.e. hydrophobic end groups) would migrate towards the membrane surface and assemble itself, thereby altering the surface features while maintaining the bulk properties of the composite membrane [6].

For the removal of hydrophobic organic HHCs, SMMs must have high affinity towards the contaminants and this can be achieved via addition of polydimethylsiloxane (PDMS) as an organophilic component [4]. Herein, two types of SMMs, terminated with hydrophobic fluoroalkanes and PDMS as soft segments, were blended with polysulfone (PSf) base polymer and tested as extractive membranes for the selective permeation of an HHC and trichloroethylene (TCE) from water. Membrane preparation was carefully controlled by varying the PDMS content in SMM, SMM content with respect to PSf, and SMM migration time to the membrane surface (air-exposure) during preparation. The performances of the composite membranes in ME were tested by measuring the TCE flux, whereas membrane structural defects were inspected through chloride leak test and various surface characterization techniques. To elucidate the differences in the composite membrane performances, TCE transport properties in pure SMM films (i.e. partition coefficient, diffusion coefficient and flux) were investigated.

2. Materials and methods

Two types of bis(3-aminopropyl), terminated PDMS with number average molecular weights ($M_n = 1,193$, 231 g/mol), were purchased from Sigma–Aldrich (Mo, USA) and Shin-Etsu Chemicals Co., Ltd. (Japan). Silicone PDMS elastomeric kit (Sylgard 184), with parts A (dimethylvinyl-terminated PDMS) and B (Pt-based catalyst cross-linking agent), was procured from Dow Corning Corporation (MI, USA). Zonyl-BAL fluorotelomer, 4,4´-Methylenebis(phenyl isocyanate) (MDI), solvents tetrahydrofuran (THF), hexane, and dimethyl acetamide (DMAc) were procured from Sigma–Aldrich (Mo, USA). PSf ($M_n = 22,000$ g/mol) was generously provided by Solvay (Korea), whereas N-methyl-2-pyrrolidone (NMP) was supplied by Showa Chemicals Co., Ltd. (Japan). Reagents for SMM synthesis were purified according to the methods described elsewhere [7].

2.1. Membrane synthesis and characterization

Fig. 1 shows the SMM synthesis scheme which involves polyurea chemistry [4]. In a moisture-free three-neck round-bottom flask, the MDI hard segment (20 mmoles) was reacted with diamine-terminated PDMS (soft segment) at 2:1 M ratio in 200 mL DMAc solvent. After 3-h reaction at 45–50℃, the oligomers were terminated with 10 mmoles of fluoroalcohol (Zonyl-BAL) for 24 h at 25℃. SMMs were recovered via precipitation and were repeatedly washed with water and finally with 20 wt% acetone/water solution. Final products were oven-dried and stored before use. Two types of SMMs were prepared: H-SMM contained PDMS component with high $M_n = 1,193$ g/mol, whereas that of L-SMM had low $M_n = 231$ g/mol.

2.1.1. Membrane film preparation

Pure SMM and PDMS films were fabricated via solvent evaporation [8]. SMMs were dissolved (3–5 wt%) in THF, whereas PDMS (10 wt%) in hexane. The dope solution was sonicated for 5 h at <40℃ (b.p. of THF). The solutions were poured on Teflon dish, covered and oven-dried (5 h at 35℃) before storage and use.
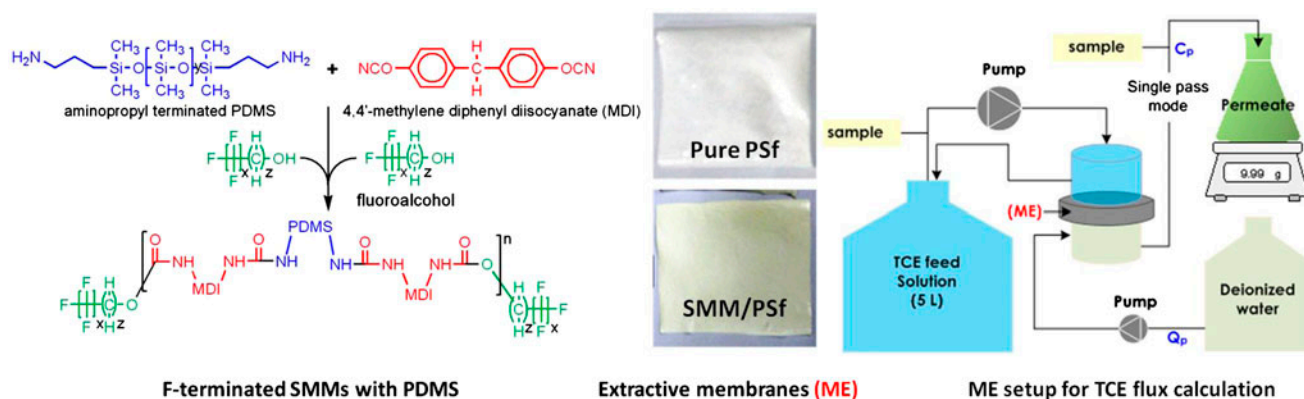
Fig. 1. SMM synthesis reaction, membrane preparation, and ME extraction setup.

2.1.2. Composite membrane preparation

Prior to blending, a desired amount of SMM was initially dissolved in THF < 40°C (H-SMM) or in NMP at 105°C (L-SMM) for 5 h. In a separate reactor, PSf dope solution was prepared in NMP solvent refluxed at 105°C. The two components were blended at 105°C for at least 3 h before it was degassed and used for membrane casting. The blends were prepared such that the final PSf concentration is 20 wt%, whereas those of SMMs were varied at 5-, 15- and 30 wt% with respect to PSf content. The prepared blend mixtures were casted on glass plates using a steel blade (200 μm gap) and the delay time (exposure to air) prior to phase inversion (i.e. immersion in water as non-solvent) were varied from 0 to 10 min. The membranes were soaked in water before use.

2.1.3. Characterization techniques

The molecular weights of SMMs were determined by gel permeation chromatography (GPC Agilent 1100 LC—RID). Solvent NMP pre-treated in 0.02 M P_2O_5 was used as the mobile phase (1 mL/min flow rate); samples were dissolved in THF and polystyrene was used as the standard. To confirm the SMM presence on the surface of PSf, Fourier-transform infrared spectrometry (FT-IR) was performed using Scimitar 2000 (Varian, USA). Hydrophobicity of the membrane samples were compared in terms of contact angle measurement [8,9]. The morphology of the membranes were inspected using field emission-scanning electron microscope (FE-SEM JSM-7000F) at 10–20 kV acceleration voltage, viewed at different magnifications.

2.2. TCE-ME permeation experiments

TCE permeation setup is illustrated in Fig. 1; experimental runs were conducted in a fibreglass ME cell which was divided into the feed and the permeate chambers, each with $V = 50$ mL capacity. The 12.57 cm² circular membrane was sandwiched between the two chambers and fixed by Teflon O-rings. The permeation was performed by a single pass of DI water at receiving permeate stream (i.e. flow rates between 10- and 50 mL/min), whereas TCE at various concentrations were re-circulated at the feed side of the reactor ($V = 5$–10 L). Both streams were delivered via peristaltic pumps. Samples at the feed and permeate outlet streams were collected periodically for TCE analysis via GC-μECD.

2.3. Analytical methods and calculations

2.3.1. Analysis

TCE concentration was measured according to the Standard Methods (No. 6232) using GC-μECD detector (HP 6980) equipped with GC 7673 autosampler and HP-5 column, [10]. Liquid–liquid extraction was performed as pre-derivatization step using n-pentane as extractant. Under splitless mode, the GC was supplied with high purity, He as carrier gas, and N_2 as make-up gas. Inlet and detector temperatures were kept at 125 and 290°C, respectively. Oven temperature was ramped from 40°C at 1°C/min to 50°C with 1 min post-run at 130°C.

2.3.2. Calculations

The intrinsic transport properties of SMMs were determined by measuring the TCE affinity towards the pure SMM films in terms of the partition coefficient parameter (K_p) as shown in Eq. (1) wherein C are aqueous (aq) TCE concentration at initial contact time ($t = 0$) and at equilibrium (equil), whereas V are the membrane (mem) and aqueous solution (solution)

volumes. The K_p values of aqueous TCE in contact with the films were determined based on a method described elsewhere [5]. Diffusion coefficients (D) were measured using Eq. (2), following the lag-time method (t_{lag}) described elsewhere, with z as the film thickness [11]. Permeability (Perm) was calculated according to Eq. (3) [12].

$$\left(\frac{C_{t=0}}{C_{equil}}\right)_{aq} - 1 = K_p \times \left(\frac{V_{mem}}{V_{solution}}\right) \tag{1}$$

$$t_{Lag} = \frac{z^2}{6D} \tag{2}$$

$$Perm = K_p \times D \tag{3}$$

$$F = \frac{C_p \times Q_p}{A} \tag{4}$$

Solute mass fluxes (F) were measured according to Eq. (4) wherein C_p is the permeate concentration, Q is permeate volumetric flow rate, and A is the membrane area. Mass fluxes were measured at steady-state condition or at constant rate of TCE permeation; for single pass of DI water at the permeate stream (i.e. continuous replenishment), steady-state condition is attained when similar or constant C_p values are obtained. All average values reported were from two to three measurements or permeation runs.

3. Results and discussion

Two types of SMMs were synthesized: according to the GPC analysis, H-SMM is a longer macromolecule with $M_n = 40{,}000$ g/mol, polydispersity ($P = 1.45$) and MDI-PDMS repeating units of 32 (n in Fig. 1). L-SMM, which has shorter PDMS segment with $M_n = 1{,}603$, $P = 1.21$, and $n = 2$. Between the two SMMs, H-SMM had higher PDMS content (84%), whereas L-SMM only had around 20%.

3.1. Selection of suitable SMM as blending component

Initial experiments were performed using pure SMM films (Fig. 2(A)) to determine their intrinsic properties of TCE extractability and diffusivity. For TCE transport to occur, the initial criteria considered is the high TCE affinity towards the SMM film as indicated by a high K_p value [5]. Fig. 2(B) shows the plots constructed according to Eq. (1); K_p values were calculated as the slopes. H-SMM exhibited higher TCE uptake than L-SMM with K_p values of 178 and 53, respectively.

Compared to K_p of aqueous TCE in pure PDMS ($K_p \cong 250$), from an early report, K_p values of both
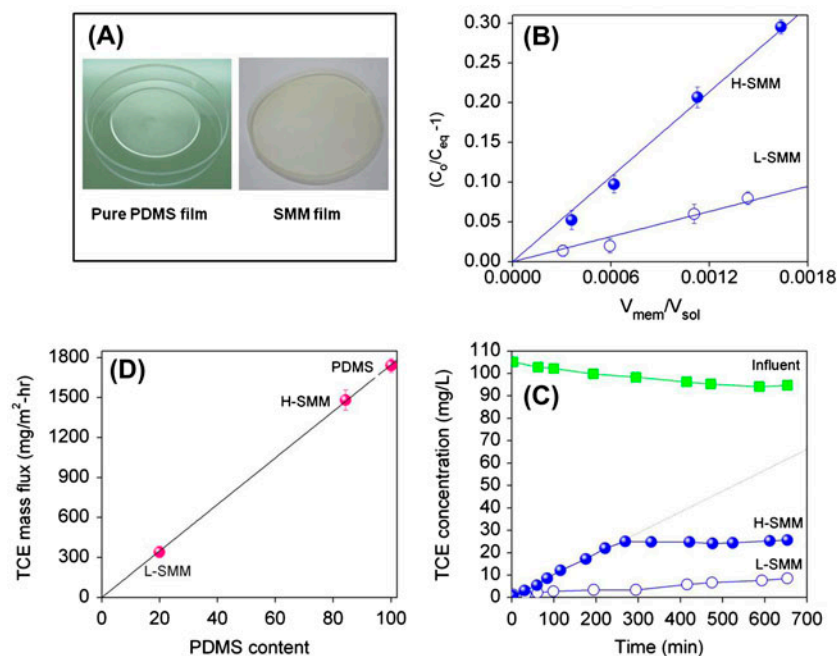

Fig. 2. TCE transport properties of SMM films (H- and L-SMM) as compared to pure PDMS.

Table 1
Transport properties of TCE through SMMs

SMM type	Density (g/cm^3)	Lag-time method		Transport parameters		
		t_{lag} (min)	Thickness (μm)	$D \times 10^{-13}$ (m^2/s)	K_p	Perm $\times 10^{-11}$ (m^2/s)
H-SMM	1.06	10.3 ± 0.50	60 ± 1.3	9.73 ± 0.84	178 ± 9.7	17.3 ± 1.77
L-SMM	1.08	10.9 ± 0.40	56 ± 2.1	8.03 ± 0.92	53 ± 7.2	4.3 ± 0.76

SMMs correspond well with their respective PDMS contents [13]. This indicates that organophilic PDMS was the responsible component in SMMs for the extractability of TCE. This explains the higher TCE K_p value in H-SMM than in L-SMM. Likewise, diffusivity experiments in Fig. 2(C) reveals lower t_{lag} value hence the faster TCE permeation in H-SMM than in L-SMM.

As expected, higher TCE Perm and flux were measured from H-SMM than from L-SMM. To further elucidate the results, TCE flux values were plotted in Fig. 2(D) against PDMS content in the SMM films. Pure PDMS served as the basis for the maximum attainable TCE flux. Results show that TCE fluxes in SMM films were strongly proportional with their PDMS content. Thus, between the two SMMs, the superior TCE transport properties of H-SMM make it a better blending agent than L-SMM. Table 1 summarizes the TCE transport properties in the two SMM films.

3.2. Composite H-SMM/PSf membrane for TCE permeation

It is known that polymeric blends with incompatible components have de-mixing tendencies caused by thermodynamic instability [7]. To reduce the stress of the system, blends of PSf and SMM have the propensity to phase separate. Previous reports indicate that components with lower surface energy (i.e. hydrophobic end groups of fluoroalkanes in SMMs) will equilibrate itself at the air phase during casting of the blend
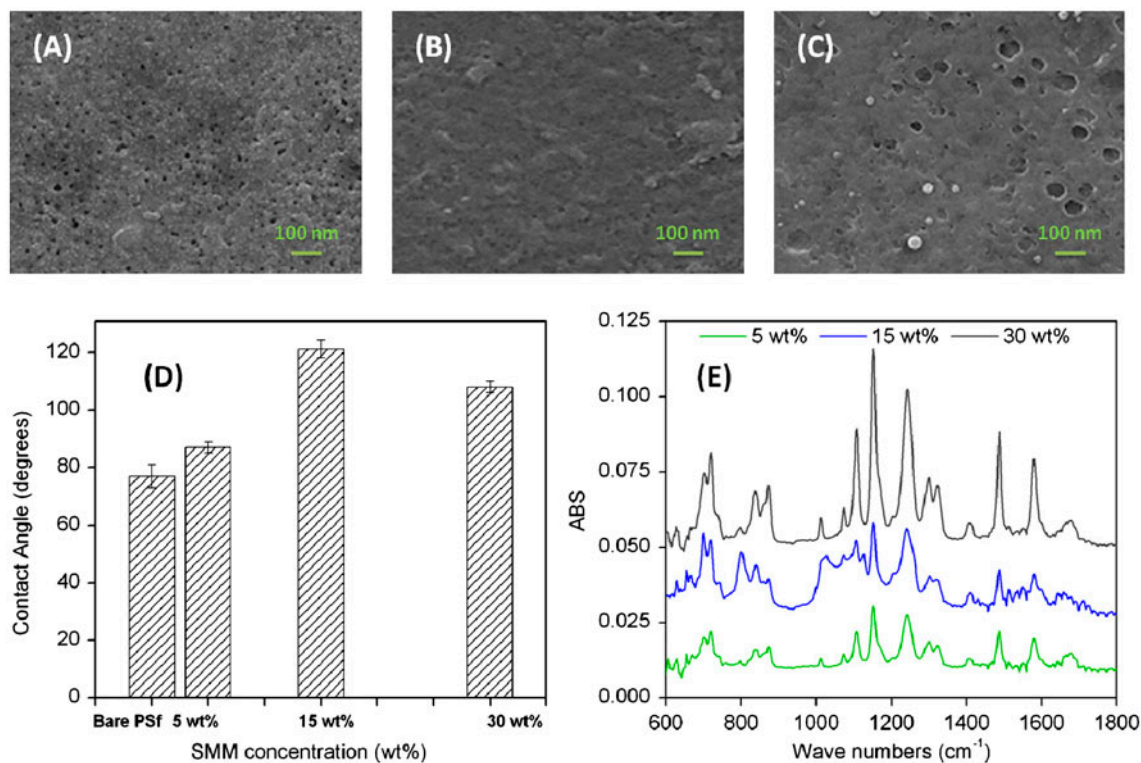

Fig. 3. Composite H-SMM/PSf membrane preparation at H-SMM contents air-exposed at 1 min. FE-SEM surface images of composite PSf with H-SMM at: (A) 5 wt%, (B) 15 wt%, (C) 30 wt%, (D) contact angle, and (E) FTIR of membrane surfaces.

solution, driving the SMM to migrate towards the membrane surface, resulting in an increase of the surface water contact angle [6]. As the SMM contains organophilic PDMS as soft segment, the surface of the membrane would become more organophilic, thereby enhancing the surface affinity of the composite membrane towards TCE. With H-SMM as the preferred blending agent, its compatibility and ability to form as a selective layer on the membrane surface was optimized to maximize TCE transport.

3.2.1. Effect of H-SMM content

Surface characteristics of composite membranes, prepared with different H-SMM contents pre-exposed to air for 1 min are shown in Fig. 3. Fig. 3(A)–(C) of FE-SEM images reveal the closure of surface pores of the composite membranes as the H-SMM content was increased. Pores were still evident at 5 wt% but disappeared at H-SMM ≥ 15 wt%, indicating the formation of H-SMM layer on the surface of the membrane. Increase in water contact angle was observed as the H-SMM concentration was increased up to 15 wt%, suggesting surface hydrophobicity improvements of the surface of composite membranes. However, slight decline was observed when H-SMM content was further increased to 30 wt%. FTIR spectra (Fig. 3(E)) reveal the increase in peak intensities which are characteristic of PDMS components (Si–C rocking and stretching at 785–815 cm^{-1}; Si–O stretching at 825–920 cm^{-1}; wagging of CH_2 in Si–C bond at 1,015–1,150 cm^{-1}; Si-CH_3 deformation at 1,245–1,270 cm^{-1}) and fluorine end groups (C–F stretching at 1,400, 1,345, and 1,300 cm^{-1}) as the H-SMM content was increased [14,15]. But at 30 wt%, intensities of PSf characteristic peaks (O=S=O at 1,050 cm^{-1}; C=C at 1,620 cm^{-1}) were also increased [16]. This indicates the insufficient amount of H-SMM present on the membrane surface. The obtained results from composite PSf with 30 wt% H-SMM is consistent with the sloughing of extremely thin films observed during phase inversion (membrane formation). At 30 wt% H-SMM, the layer probably became thick enough that it was able to detach itself from the bulk base polymer upon immersion in the non-solvent bath. This could explain the lack of SMM presence in some parts of the 30 wt% H-SMM/PSf membrane surface.

3.2.2. Effect of H-SMM content on TCE permeation of the composite PSf membrane

The presence of surface defects on composite PSf with 5 and 30 wt% H-SMM were further confirmed by TCE permeation results in Fig. 4. Fig. 4(A) reveals that among the membranes tested, PSf with 30 wt%
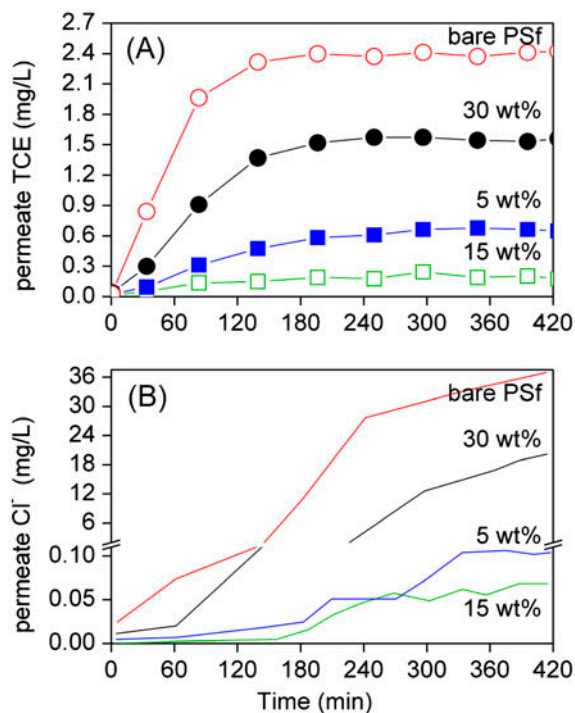

Fig. 4. TCE permeation experiments using H-SMM/PSf composite membrane with different H-SMM loading (A) TCE permeate concentration and (B) membrane leak test using Cl^- as probing solute. [TCE feed] = 19.8 ± 1.3 mg/L; [Cl^- feed] = 50 mg/L.

H-SMM showed the highest TCE permeation closest to that of the bare porous PSf in which TCE permeated through the pores of the membrane. The "defects" (pores) which were revealed when the H-SMM layer was sloughed off could explain the high TCE flux at 30 wt% H-SMM. Likewise, the higher TCE flux in 5 wt% H-SMM could be due to the incomplete H-SMM layer formation as evidenced by the pores in Fig. 3(A). The passage of TCE through the pores of 5 and 30 wt% H-SMM/PSf was confirmed by chloride leak test result in Fig. 4(B). A saline solution was used as a feed instead of TCE. PSf with 30 wt% H-SMM had significantly higher Cl^- leakage (i.e. comparable with that of the bare porous PSf) followed by 5 wt%, whereas that of 15 wt% H-SMMs had negligible [Cl^-]. Thus, based on the characterization and permeation results, composite membrane with 15 wt% H-SMM provided the best results and was therefore selected for further experiments.

3.2.3. Effect of air-exposure time

The period of delay after the blend solution is casted on the glass plate prior to membrane formation is critical, to determine the optimum migration period of the
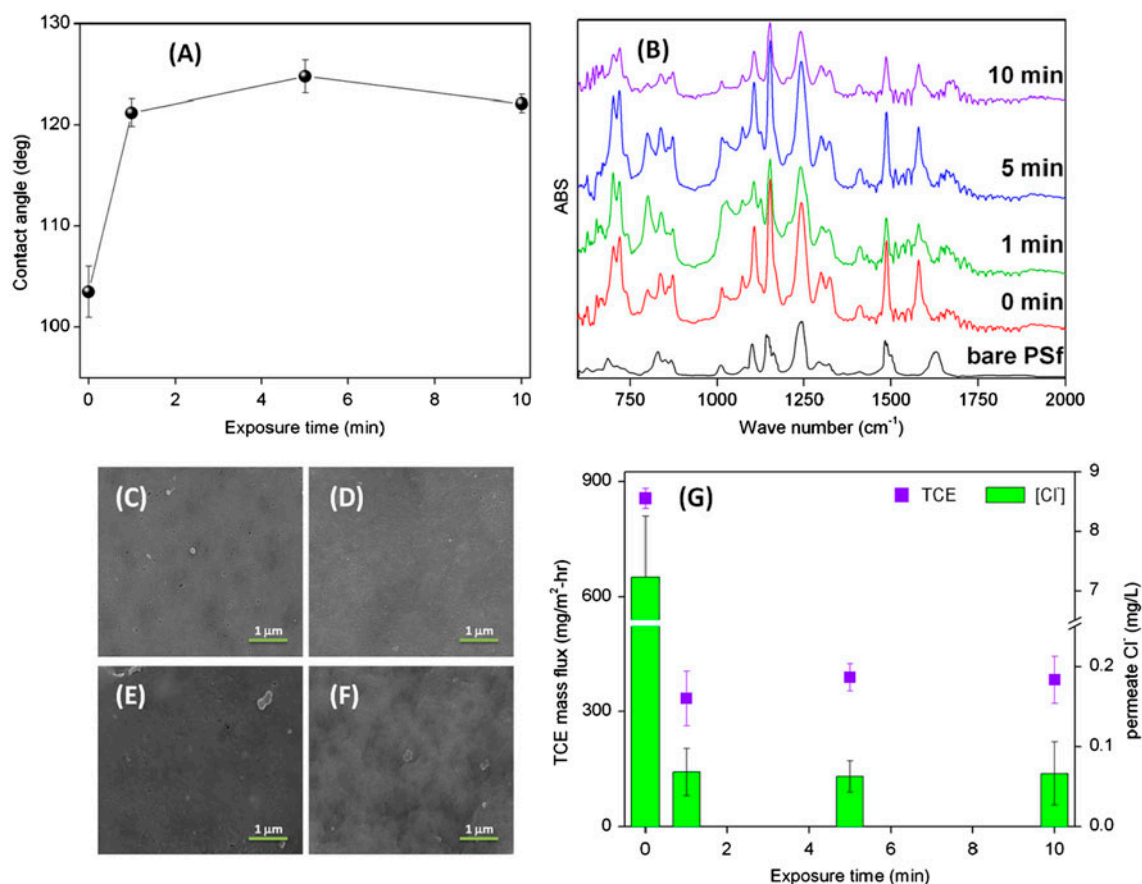
Fig. 5. Composite (5 wt% H-SMM) PSf membrane preparation at different air-exposure times. (A) Contact angle, (B) FTIR of membrane surface; FE-SEM surface images, (C) 0 min, (D) 1 min, (E) 5 min, (F) 10 min air-exposure time, and (G) TCE permeation test and membrane leak test. [TCE feed] = 19.91 ± 1.1 mg/L; [Cl⁻ feed] = 50 mg/L.

H-SMMs towards the surface of the membrane [7]. Fig. 5(A) reveals the gradual increase in contact angle up to 5 min of air-exposure and no significant increase at 10 min. FTIR spectra in Fig. 5(B) reveals similar characteristic peaks as observed in Fig. 3(B) for samples containing 15 wt% of H-SMM which indicates the presence of PDMS and F-groups of H-SMMs on the surface of composite membranes [14,15]. Fig. 5(C)–(F) reveals the gradual surface morphological transformation of the membranes with increasing delay period; with longer air-exposure, the surface appeared to have less pores but with softer appearance. Results indicate that as delay period was prolonged, more H-SMM was allowed to form itself on the composite membrane surface.

3.2.4. Effect of air-exposure time on TCE permeation of the composite PSf membrane

Short period of air-exposure may result in incomplete de-mixing and presence of significant pores which could channel the feed solution to the permeate stream. On the other hand, extended delay period could lead to thick H-SMM layer formation (i.e. sloughing problem) or evaporation of solvent in the casted solution; a very thick nonporous membrane could form and therefore, the membrane resistance for TCE transport would be undesirably increased. The high TCE flux of sample prepared with zero air-exposure time in Fig. 5(G) was due to TCE transport through the membrane pores as it exhibited high leakage of Cl⁻. On the other hand, membranes exposed ≥ 1 min had negligible permeate [Cl⁻], which further affirms the necessity of air-exposure time to facilitate efficient H-SMM layer formation on the membrane surface. Highest TCE fluxes were measured at ≥5 min. Thus, for practical reasons, air-exposure time was set at 5 min since beyond this period, similar membrane surface attributes and transport behaviors were observed.

3.2.5. TCE permeation in selected H-SMM/PSf composite membrane

Using the composite membrane of PSf with 15 wt% H-SMM air-exposed for 5 min prior to phase inversion,
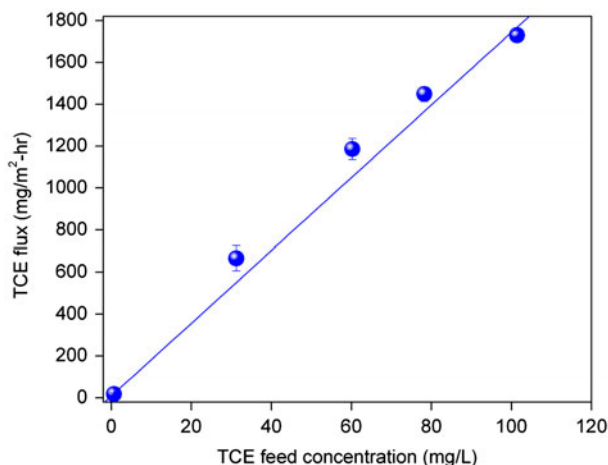
Fig. 6. TCE flux at different feed concentrations (15 wt% H-SMM/PSf and 5 min exposure time).

TCE permeation was performed at different feed concentrations as shown in Fig. 6. TCE flux was observed to be proportional to the feed concentration which could be due to the increase in driving force or concentration gradient across the membrane [5]. Using the selected composite membrane, TCE flux between 640 and 1,790 mg/m^2 h can be obtained for feed concentrations between 30 and 105 mg TCE/L. Previous reports on PV of TCE using various organophilic membranes exhibited high flux values (>7,000 mg/m^2 h); this is understandable as PV is governed by vapor pressure gradient (i.e. pressure-driven), whereas ME process relies on the TCE concentration difference [17]. Nonetheless, ME is a very simple and low energy-requiring process as compared to PV. Furthermore, ME can be easily combined with other permeate processes which makes complete TCE degradation possible, a great advantage over PV systems [5].

4. Conclusions

A composite membrane made of PSf with SMM containing organophilic PDMS as soft segment was successfully prepared, characterized, and optimized. Factors such as SMM type, SMM content in the base polymer, and exposure time of casted membrane before membrane formation were critical in obtaining a composite membrane with minimal surface defects and high affinity towards the target compound TCE. Overall, the proposed process of using a composite organophilic membrane containing H-SMM in PSf can be used in a facile, energy-efficient process like the ME system for the separation of organic and hydrophobic contaminants such as TCE from water.

References

[1] K. Gopal, S.S. Tripathy, J.L. Bersillon, S.P. Dubey, Chlorination byproducts, their toxicodynamics and removal from drinking water, J. Hazard. Mater. 140 (2007) 1–6.
[2] H. Mahmud, J. Minnery, Y. Fang, V.A. Pham, R.M. Narbaitz, J.P. Santerre, T. Matsuura, Evaluation of membranes containing surface modifying macromolecules: Determination of the chloroform separation from aqueous mixtures via pervaporation, J. Appl. Polym. Sci. 79 (2001) 183–189.
[3] M. Khayet, T. Matsuura, Application of surface modifying macromolecules for the preparation of membranes for membrane distillation, Desalination 158 (2003) 51–56.
[4] D.E. Suk, T. Matsuura, H.B. Park, Y.M. Lee, Synthesis of a new type of surface modifying macromolecules (nSMM) and characterization and testing of nSMM blended membranes for membrane distillation, J. Membr. Sci. 277 (2006) 177–185.
[5] P.R. Brookes, A.G. Livingston, Aqueous–aqueous extraction of organic pollutants through tubular silicone rubber membranes, J. Membr. Sci. 104 (1995) 119–137.
[6] M. Khayet, T. Matsuura, Surface modification of membranes for the separation of volatile organic compounds from water by pervaporation, Desalination 148 (2002) 31–37.
[7] D.E. Suk, G. Chowdhury, T. Matsuura, R.M. Narbaitz, P. Santerre, G. Pleizier, Y. Deslandes, Study on the kinetics of surface migration of surface modifying macromolecules in membrane preparation, Macromolecules 35 (2002) 3017–3021.
[8] G.M. Nisola, A.B. Beltran, D.M. Sim, D.J. Lee, B. Jung, W.-J. Chung, Dimethyl silane-modified silica in polydimethylsiloxane as gas permeation mixed matrix membrane, J. Polym. Res. 18 (2011) 2415–2424.
[9] T. Gumí, M. Valiente, K.C. Khulbe, C. Paelt, T. Matsuura, Characterization of activated composite membranes by solute transport, contact angle measurement, AFM and ESR, J. Membr. Sci. 212 (2003) 123–134.
[10] APHA, AWWA, WEF, Standard Methods for the Examination of Water and Wastewater, 21st ed., American Public Health Association, Washington, DC, USA, 2005, 6-40–6-46.
[11] A. Oztan, M. Mutlu, Mass transfer through meat. Part I. Determination of diffusion coefficient of nitrite by time lag method, J. Food Eng. 67 (2005) 387–391.
[12] G.M. Nisola, E.S. Cho, A.B. Beltran, M. Han, Y. Kim, W.-J. Chung, Dye/water separation through supported liquid membrane extraction, Chemosphere 80 (2010) 894–900.

[13] B. Zimmermann, J. Bürck, H.-J. Ache, Studies on siloxane polymers for NIR-evanescent wave absorbance sensors, Sens. Actuators B 41 (1997) 45–54.

[14] P. Zelenay, M.A. Habib, J.O'.M. Bockris, Adsorption of trifluoromethane sulfonic acid on Pt by FTIR and radiotracer methods, J. Electrochem. Soc. 131 (1984) 2464–2465.

[15] E. Kirill, W.E. Wallace, J. Genzer, Surface modification of Sylgard-184 poly(dimethyl siloxane) networks by ultraviolet and ultraviolet/ozone treatment, J. Colloid Interface. Sci. 254 (2002) 306–315.

[16] G.M. Nisola, J.S. Park, A.B. Beltran, W.-J. Chung, Silver nanoparticles in a polyether-block-polyamide copolymer towards antimicrobial and antifouling membranes, RSC Adv. 2 (2012) 2439–2448.

[17] M. Peng, L.M. Vane, S.X. Liu, Recent advances in VOCs removal from water by pervaporation, J. Hazard. Mater. B98 (2003) 69–90.